*Environ Health Perspect*
DOI: 10.1289/EHP742



# Supplemental Material

# A High-Throughput Analysis of Ovarian Cycle Disruption by Mixtures of Aromatase Inhibitors

Frederic Y. Bois, Nazanin Golbamaki-Bakhtyari, Simona Kovarich, Cleo Tebby, Henry A. Gabb, and Emmanuel Lemazurier

## Table of Contents

**Figure S1:** Computational workflow.

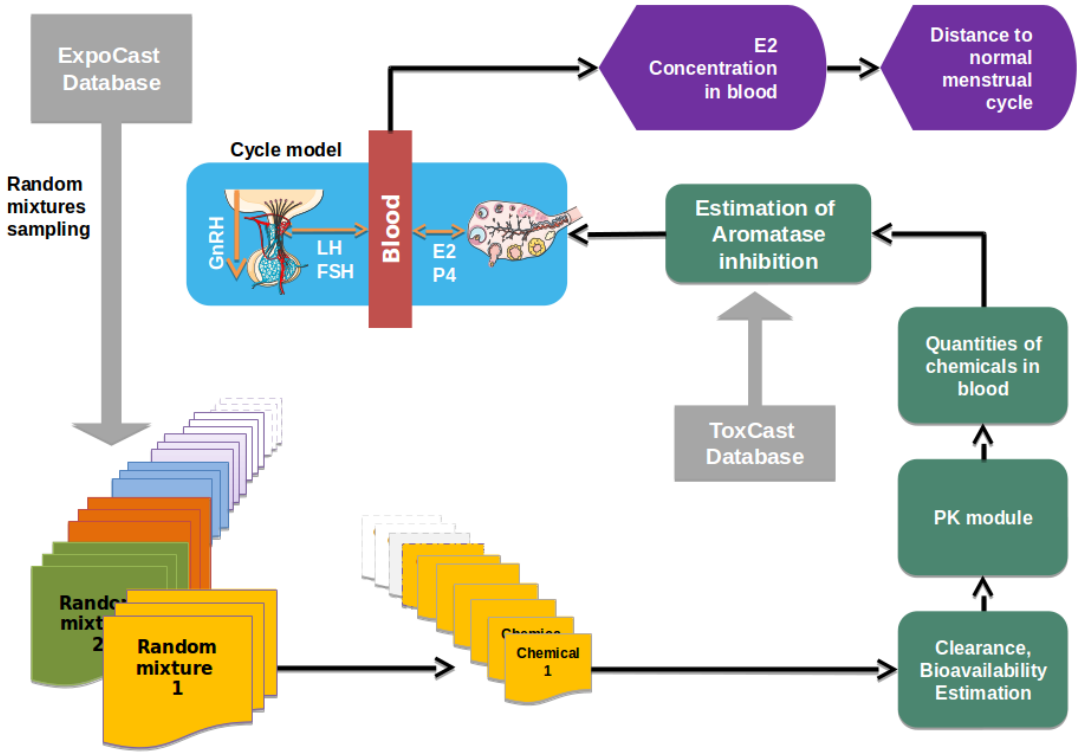


**Figure S1.** Computational workflow. Each box represents a task to be executed or a result obtained and arrows represent either data flow or execution dependencies between different tasks. Random mixtures of chemicals are sampled from ExpoCast. The kinetics of each chemical in the human body are computed using a one-compartment PK model. The resulting aromatase inhibition is computed from ToxCast dose-response information. The impact of that inhibition on the menstrual cycle is estimated using an ovarian cycle model adapted from Chen and Ward (2013).

**Methods S1:** PK modules of ACD/Labs.

**The ACD/Oral Bioavailability module** uses a combination of probabilistic and mechanistic models to predict oral bioavailability based on a dataset of oral bioavailability data for 788 substances. The module predicts the fraction of the specified dose that reaches systemic circulation after oral administration (*F*), with the possibility to explore dose-dependence of *F*. The default oral dose used in calculations is 50 mg. The mathematical model used for simulations in the Oral Bioavailability (and PK Explorer) modules is based on differential equations that consider solubility in the gastrointestinal tract, passive-absorption in jejunum, elimination (total body clearance), and volume of distribution. Simulations performed with the Oral Bioavailability module ignore first-pass metabolism in liver and gut. Quantitative *F* values are calculated as a ratio of AUCs after oral and intravenous administration. A number of endpoints affecting oral bioavailability are also predicted, including solubility (dose/solubility ratio), stability in acidic media, intestinal membrane permeability by passive or active transport (with a summary of transporters where relevant), P-gp efflux (multi-drug transporter P-glycoprotein) and first pass metabolism in the liver. For the majority of these parameters, ACD/Labs Percepta allows the user to assesses the confidence in the predicted result by means of reliability index and/or displaying similar structures from the training set along with their experimental test results. Since the bioavailability predictions are based on a mechanistic simulation model rather that statistical fitting to data, the validation procedure was not based on a conventional training/test set approach. Instead, a set of clinical fraction absorbed ($f_a$) data together with dosage information for 28 drugs reported by Parrot and Lavé (2002) was used for validation purposes. The model performance was assessed qualitatively, by evaluating the accuracy of three-class classification (i.e., "low" for $f_a \leq 33\%$, "moderate" for $33\% < f_a < 66\%$, "high" for $f_a \geq 66\%$), and quantitatively, using the Residual Mean Square Error statistic and visual inspection of the correlation between observed and predicted $f_a$ values for the drugs considered. For the majority of drugs, calculated values were in good agreement with clinical data, resulting in 80% correct classification and an RMSE equal to 17%.

**ACD/PK Explorer** is a tool for exploring pharmacokinetic relationships (*e.g.*, *F*–Dose relationship) using physico-chemical parameters as inputs for calculations. Total body clearance rate constant (*Ke*) is among the required parameters of our PK model. *Ke was* estimated using a set of fragmental ionization class specific models. Hydrophobicity (logP) and ionization (pKa) are the principal descriptors for the prediction of *Ke*. These descriptors were calculated *in silico*. Technical details on those models and equations are not available since they are proprietary information of ACD/Labs.

**Figure S1:** Predictions of bioavailability ($F$) and total body clearance rate constant ($K_e$). The ACD/Labs Percepta Oral Bioavailability module was used for predictions of oral F values. F predictions depend on oral dose and are given for an array of doses. The module ACD/ PK Explorer was used for the prediction of $K_e$ values.

| ID | CAS | F (0.001 mg) | F (0.01 mg) | F (0.1 mg) | F (1 mg) | F (5 mg) | F (10 mg) | F (50 mg) | F (100 mg) | F (500 mg) | F (1000 mg) | $K_e$ ($min^{-1}$) |
|---|---|---|---|---|---|---|---|---|---|---|---|---|
| 1 | 101-20-2 | 0.2805 | 0.2804 | 0.2798 | 0.2739 | 0.2505 | 0.2269 | 0.1342 | 0.0919 | 0.0295 | 0.0168 | 0.00083 |
| 2 | 101-80-4 | 0.9760 | 0.9760 | 0.9760 | 0.9759 | 0.9754 | 0.9748 | 0.9661 | 0.9486 | 0.5863 | 0.3625 | 0.002 |
| 3 | 112281-77-3 | 0.9907 | 0.9907 | 0.9907 | 0.9907 | 0.9903 | 0.9899 | 0.9826 | 0.9575 | 0.5201 | 0.3202 | 0.0011 |
| 4 | 112809-51-5 | 0.9919 | 0.9919 | 0.9919 | 0.9919 | 0.9917 | 0.9915 | 0.9880 | 0.9771 | 0.6065 | 0.3808 | 0.00041 |
| 5 | 114369-43-6 | 0.7271 | 0.7270 | 0.7261 | 0.7175 | 0.6807 | 0.6385 | 0.4214 | 0.2983 | 0.0986 | 0.0566 | 0.0011 |
| 6 | 115-39-9 | 0.2164 | 0.2164 | 0.2158 | 0.2104 | 0.1897 | 0.1694 | 0.0956 | 0.0644 | 0.0201 | 0.0114 | 0.00087 |
| 7 | 116255-48-2 | 0.9884 | 0.9884 | 0.9884 | 0.9882 | 0.9872 | 0.9856 | 0.9580 | 0.8774 | 0.3949 | 0.2374 | 0.0011 |
| 8 | 117-39-5 | 0.9533 | 0.9533 | 0.9533 | 0.9532 | 0.9528 | 0.9521 | 0.9429 | 0.9247 | 0.5982 | 0.3723 | 0.0062 |
| 9 | 1192-52-5 | 0.9942 | 0.9942 | 0.9942 | 0.9942 | 0.9942 | 0.9942 | 0.9942 | 0.9942 | 0.9938 | 0.9933 | 0.0015 |
| 10 | 120511-73-1 | 0.9916 | 0.9916 | 0.9916 | 0.9916 | 0.9915 | 0.9915 | 0.9910 | 0.9901 | 0.9455 | 0.7218 | 0.0009 |
| 11 | 125-84-8 | 0.9936 | 0.9936 | 0.9936 | 0.9936 | 0.9936 | 0.9936 | 0.9935 | 0.9932 | 0.9899 | 0.9812 | 0.0019 |
| 12 | 126-72-7 | 0.9908 | 0.9908 | 0.9908 | 0.9907 | 0.9904 | 0.9899 | 0.9826 | 0.9586 | 0.5198 | 0.3193 | 0.0012 |
| 13 | 126-86-3 | 0.9938 | 0.9938 | 0.9938 | 0.9938 | 0.9937 | 0.9935 | 0.9915 | 0.9862 | 0.6964 | 0.4480 | 0.0017 |
| 14 | 1260-17-9 | 0.0078 | 0.0078 | 0.0078 | 0.0078 | 0.0078 | 0.0078 | 0.0078 | 0.0078 | 0.0078 | 0.0078 | 0.0049 |
| 15 | 129-17-9 | 0.0000 | 0.0000 | 0.0000 | 0.0000 | 0.0000 | 0.0000 | 0.0000 | 0.0000 | 0.0000 | 0.0000 | 0.0071 |
| 16 | 129453-61-8 | 0.0067 | 0.0067 | 0.0066 | 0.0064 | 0.0056 | 0.0049 | 0.0026 | 0.0017 | 0.0005 | 0.0003 | 0.0002 |
| 17 | 131341-86-1 | 0.9393 | 0.9393 | 0.9390 | 0.9360 | 0.9223 | 0.9039 | 0.7408 | 0.5798 | 0.2155 | 0.1264 | 0.0002 |
| 18 | 13171-00-1 | 0.9836 | 0.9836 | 0.9835 | 0.9830 | 0.9802 | 0.9759 | 0.9089 | 0.7791 | 0.3177 | 0.1886 | 0.0012 |
| 19 | 131860-33-8 | 0.9603 | 0.9603 | 0.9601 | 0.9581 | 0.9481 | 0.9337 | 0.7802 | 0.6097 | 0.2225 | 0.1298 | 0.00068 |

| ID | CAS | F (0.001 mg) | F (0.01 mg) | F (0.1 mg) | F (1 mg) | F (5 mg) | F (10 mg) | F (50 mg) | F (100 mg) | F (500 mg) | F (1000 mg) | $K_e$ ($min^{-1}$) |
|---|---|---|---|---|---|---|---|---|---|---|---|---|
| 20 | 13292-46-1 | 0.1755 | 0.1755 | 0.1755 | 0.1755 | 0.1755 | 0.1755 | 0.1755 | 0.1755 | 0.1754 | 0.1713 | 0.0019 |
| 21 | 133-06-2 | 0.8723 | 0.8723 | 0.8717 | 0.8665 | 0.8427 | 0.8128 | 0.6083 | 0.4543 | 0.1600 | 0.0930 | 0.0017 |
| 22 | 133-07-3 | 0.5715 | 0.5714 | 0.5705 | 0.5623 | 0.5282 | 0.4910 | 0.3167 | 0.2236 | 0.0742 | 0.0427 | 0.0015 |
| 23 | 133855-98-8 | 0.9064 | 0.9064 | 0.9059 | 0.9016 | 0.8814 | 0.8551 | 0.6557 | 0.4932 | 0.1743 | 0.1012 | 0.00075 |
| 24 | 137-26-8 | 0.9764 | 0.9764 | 0.9763 | 0.9750 | 0.9690 | 0.9603 | 0.8526 | 0.7011 | 0.2741 | 0.1619 | 0.0022 |
| 25 | 137-30-4 | 0.8689 | 0.8689 | 0.8689 | 0.8689 | 0.8689 | 0.8689 | 0.8689 | 0.8689 | 0.8689 | 0.8689 | 0.0032 |
| 26 | 14233-37-5 | 0.8501 | 0.8500 | 0.8494 | 0.8430 | 0.8143 | 0.7789 | 0.5556 | 0.4044 | 0.1376 | 0.0794 | 0.0014 |
| 27 | 15299-99-7 | 0.9827 | 0.9827 | 0.9826 | 0.9819 | 0.9785 | 0.9734 | 0.8969 | 0.7597 | 0.3053 | 0.1809 | 0.0014 |
| 28 | 155990-20-8 | 0.9920 | 0.9920 | 0.9920 | 0.9920 | 0.9920 | 0.9920 | 0.9920 | 0.9920 | 0.9919 | 0.9915 | 0.0013 |
| 29 | 15972-60-8 | 0.9952 | 0.9952 | 0.9952 | 0.9952 | 0.9952 | 0.9952 | 0.9950 | 0.9948 | 0.9901 | 0.9624 | 0.0019 |
| 30 | 16423-68-0 | 0.0002 | 0.0002 | 0.0002 | 0.0001 | 0.0001 | 0.0001 | 0.0001 | 0.0000 | 0.0000 | 0.0000 | 0.00065 |
| 31 | 175013-18-0 | 0.9892 | 0.9892 | 0.9892 | 0.9890 | 0.9882 | 0.9870 | 0.9656 | 0.8972 | 0.4116 | 0.2477 | 0.0012 |
| 32 | 17924-92-4 | 0.9958 | 0.9958 | 0.9958 | 0.9958 | 0.9958 | 0.9958 | 0.9953 | 0.9943 | 0.9495 | 0.7248 | 0.0022 |
| 33 | 1918-02-1 | 66.39 | 66.39 | 66.39 | 66.39 | 66.39 | 66.39 | 66.39 | 66.39 | 66.39 | 66.39 | 0.0025 |
| 34 | 199171-88-5 | 0.9916 | 0.9916 | 0.9916 | 0.9916 | 0.9916 | 0.9916 | 0.9913 | 0.9909 | 0.9811 | 0.9148 | 0.00099 |
| 35 | 2310-17-0 | 0.7593 | 0.7592 | 0.7584 | 0.7503 | 0.7153 | 0.6745 | 0.4547 | 0.3245 | 0.1083 | 0.0623 | 0.0014 |
| 36 | 2312-35-8 | 0.8301 | 0.8301 | 0.8294 | 0.8223 | 0.7913 | 0.7535 | 0.5266 | 0.3800 | 0.1280 | 0.0737 | 0.0013 |
| 37 | 2353-45-9 | 0.0000 | 0.0000 | 0.0000 | 0.0000 | 0.0000 | 0.0000 | 0.0000 | 0.0000 | 0.0000 | 0.0000 | 0.0047 |
| 38 | 24169-02-6 | 0.6276 | 0.6275 | 0.6266 | 0.6173 | 0.5789 | 0.5366 | 0.3397 | 0.2372 | 0.0773 | 0.0442 | 0.00089 |
| 39 | 2425-06-1 | 0.5641 | 0.5641 | 0.5632 | 0.5544 | 0.5186 | 0.4797 | 0.3031 | 0.2121 | 0.0695 | 0.0398 | 0.0016 |
| 40 | 29091-21-2 | 0.2182 | 0.2182 | 0.2177 | 0.2127 | 0.1932 | 0.1739 | 0.1007 | 0.0685 | 0.0218 | 0.0124 | 0.00054 |
| 41 | 30399-84-9 | 0.9043 | 0.9042 | 0.9037 | 0.8990 | 0.8772 | 0.8488 | 0.6383 | 0.4740 | 0.1645 | 0.0952 | 0.0011 |

| ID | CAS | F (0.001 mg) | F (0.01 mg) | F (0.1 mg) | F (1 mg) | F (5 mg) | F (10 mg) | F (50 mg) | F (100 mg) | F (500 mg) | F (1000 mg) | $K_e$ ($min^{-1}$) |
|---|---|---|---|---|---|---|---|---|---|---|---|---|
| 42 | 311-45-5 | 0.9965 | 0.9965 | 0.9965 | 0.9965 | 0.9965 | 0.9965 | 0.9965 | 0.9964 | 0.9957 | 0.9940 | 0.0023 |
| 43 | 35554-44-0 | 0.9924 | 0.9924 | 0.9924 | 0.9924 | 0.9924 | 0.9923 | 0.9916 | 0.9903 | 0.8887 | 0.6276 | 0.0012 |
| 44 | 3844-45-9 | 0.0000 | 0.0000 | 0.0000 | 0.0000 | 0.0000 | 0.0000 | 0.0000 | 0.0000 | 0.0000 | 0.0000 | 0.007 |
| 45 | 43121-43-3 | 0.9919 | 0.9919 | 0.9919 | 0.9918 | 0.9917 | 0.9915 | 0.9889 | 0.9819 | 0.6581 | 0.4188 | 0.0012 |
| 46 | 49562-28-9 | 0.9326 | 0.9326 | 0.9322 | 0.9286 | 0.9116 | 0.8886 | 0.6955 | 0.5259 | 0.1858 | 0.1079 | 0.0016 |
| 47 | 50-41-9 | 0.9197 | 0.9197 | 0.9193 | 0.9151 | 0.8954 | 0.8692 | 0.6612 | 0.4919 | 0.1704 | 0.0986 | 0.00014 |
| 48 | 50594-66-6 | 0.6879 | 0.6878 | 0.6868 | 0.6771 | 0.6361 | 0.5904 | 0.3727 | 0.2590 | 0.0836 | 0.0477 | 0.00064 |
| 49 | 51630-58-1 | 0.0101 | 0.0101 | 0.0100 | 0.0098 | 0.0087 | 0.0077 | 0.0042 | 0.0028 | 0.0009 | 0.0005 | 0.0014 |
| 50 | 52-01-7 | 0.9256 | 0.9255 | 0.9251 | 0.9209 | 0.9011 | 0.8746 | 0.6651 | 0.4948 | 0.1714 | 0.0991 | 0.0027 |
| 51 | 520-18-3 | 0.9892 | 0.9892 | 0.9892 | 0.9892 | 0.9890 | 0.9888 | 0.9865 | 0.9819 | 0.8086 | 0.5408 | 0.0015 |
| 52 | 521-18-6 | 0.9647 | 0.9647 | 0.9645 | 0.9624 | 0.9521 | 0.9375 | 0.7852 | 0.6166 | 0.2272 | 0.1328 | 0.0036 |
| 53 | 53-16-7 | 0.9600 | 0.9600 | 0.9598 | 0.9578 | 0.9480 | 0.9342 | 0.7886 | 0.6236 | 0.2321 | 0.1360 | 0.0012 |
| 54 | 55219-65-3 | 0.9917 | 0.9917 | 0.9917 | 0.9917 | 0.9914 | 0.9910 | 0.9858 | 0.9684 | 0.5578 | 0.3462 | 0.0013 |
| 55 | 57-63-6 | 0.8500 | 0.8500 | 0.8493 | 0.8430 | 0.8149 | 0.7801 | 0.5593 | 0.4083 | 0.1395 | 0.0806 | 0.0011 |
| 56 | 577-11-7 | 0.8287 | 0.8286 | 0.8278 | 0.8198 | 0.7841 | 0.7411 | 0.4968 | 0.3509 | 0.1149 | 0.0658 | 0.0055 |
| 57 | 58-14-0 | 0.9688 | 0.9687 | 0.9686 | 0.9672 | 0.9600 | 0.9488 | 0.7915 | 0.6000 | 0.2057 | 0.1184 | 0.0014 |
| 58 | 58-89-9 | 0.9227 | 0.9227 | 0.9223 | 0.9188 | 0.9024 | 0.8808 | 0.7044 | 0.5441 | 0.1994 | 0.1167 | 0.0018 |
| 59 | 60168-88-9 | 0.8674 | 0.8673 | 0.8667 | 0.8610 | 0.8352 | 0.8027 | 0.5871 | 0.4324 | 0.1493 | 0.0864 | 0.0011 |
| 60 | 60-57-1 | 0.3142 | 0.3142 | 0.3135 | 0.3071 | 0.2819 | 0.2562 | 0.1532 | 0.1054 | 0.0339 | 0.0194 | 0.0012 |
| 61 | 62924-70-3 | 0.3046 | 0.3045 | 0.3038 | 0.2971 | 0.2707 | 0.2442 | 0.1422 | 0.0968 | 0.0307 | 0.0175 | 0.00024 |
| 62 | 633-96-5 | 0.7686 | 0.7686 | 0.7686 | 0.7686 | 0.7686 | 0.7686 | 0.7684 | 0.7681 | 0.7457 | 0.6995 | 0.0027 |

| ID | CAS | F (0.001 mg) | F (0.01 mg) | F (0.1 mg) | F (1 mg) | F (5 mg) | F (10 mg) | F (50 mg) | F (100 mg) | F (500 mg) | F (1000 mg) | $K_e$ ($min^{-1}$) |
|---|---|---|---|---|---|---|---|---|---|---|---|---|
| 63 | 643-79-8 | 0.9938 | 0.9938 | 0.9938 | 0.9938 | 0.9938 | 0.9938 | 0.9938 | 0.9938 | 0.9934 | 0.9929 | 0.0014 |
| 64 | 6459-94-5 | 0.0000 | 0.0000 | 0.0000 | 0.0000 | 0.0000 | 0.0000 | 0.0000 | 0.0000 | 0.0000 | 0.0000 | 0.00093 |
| 65 | 6610-29-3 | 0.4977 | 0.4977 | 0.4977 | 0.4977 | 0.4977 | 0.4977 | 0.4977 | 0.4977 | 0.4953 | 0.4840 | 0.0024 |
| 66 | 6625-46-3 | 0.0001 | 0.0001 | 0.0001 | 0.0001 | 0.0001 | 0.0001 | 0.0001 | 0.0001 | 0.0001 | 0.0001 | 0.0034 |
| 67 | 67-20-9 | 0.9912 | 0.9912 | 0.9912 | 0.9912 | 0.9911 | 0.9910 | 0.9898 | 0.9875 | 0.9150 | 0.6701 | 0.0016 |
| 68 | 67747-09-5 | 0.9904 | 0.9904 | 0.9903 | 0.9902 | 0.9896 | 0.9888 | 0.9742 | 0.9245 | 0.4481 | 0.2716 | 0.0013 |
| 69 | 68-26-8 | 0.9807 | 0.9807 | 0.9806 | 0.9799 | 0.9762 | 0.9706 | 0.8870 | 0.7427 | 0.2928 | 0.1729 | 0.0011 |
| 70 | 68694-11-1 | 0.9918 | 0.9918 | 0.9918 | 0.9918 | 0.9917 | 0.9916 | 0.9899 | 0.9856 | 0.7227 | 0.4689 | 0.00044 |
| 71 | 79241-46-6 | 0.9150 | 0.9150 | 0.9145 | 0.9103 | 0.8906 | 0.8646 | 0.6624 | 0.4965 | 0.1742 | 0.1010 | 0.0011 |
| 72 | 84-61-7 | 0.9670 | 0.9670 | 0.9668 | 0.9648 | 0.9553 | 0.9415 | 0.7935 | 0.6247 | 0.2304 | 0.1347 | 0.0029 |
| 73 | 85509-19-9 | 0.9813 | 0.9813 | 0.9812 | 0.9805 | 0.9771 | 0.9718 | 0.8933 | 0.7539 | 0.3011 | 0.1782 | 0.00051 |
| 74 | 86-50-0 | 0.9902 | 0.9902 | 0.9902 | 0.9899 | 0.9883 | 0.9860 | 0.9459 | 0.8454 | 0.3659 | 0.2190 | 0.002 |
| 75 | 872-50-4 | 0.9959 | 0.9959 | 0.9959 | 0.9959 | 0.9959 | 0.9959 | 0.9959 | 0.9959 | 0.9959 | 0.9959 | 0.0022 |
| 76 | 87392-12-9 | 0.9951 | 0.9951 | 0.9951 | 0.9951 | 0.9951 | 0.9951 | 0.9948 | 0.9944 | 0.9835 | 0.8928 | 0.0019 |
| 77 | 87674-68-8 | 0.9960 | 0.9960 | 0.9960 | 0.9960 | 0.9960 | 0.9960 | 0.9959 | 0.9959 | 0.9952 | 0.9936 | 0.0021 |
| 78 | 88-58-4 | 0.9925 | 0.9925 | 0.9925 | 0.9924 | 0.9924 | 0.9923 | 0.9916 | 0.9901 | 0.8756 | 0.6122 | 0.0012 |
| 79 | 88671-89-0 | 0.9916 | 0.9916 | 0.9916 | 0.9914 | 0.9905 | 0.9892 | 0.9648 | 0.8909 | 0.4072 | 0.2453 | 0.0019 |
| 80 | 88-72-2 | 0.9955 | 0.9955 | 0.9955 | 0.9955 | 0.9955 | 0.9955 | 0.9954 | 0.9952 | 0.9906 | 0.9465 | 0.0019 |
| 81 | 88-85-7 | 0.9950 | 0.9950 | 0.9950 | 0.9950 | 0.9950 | 0.9950 | 0.9950 | 0.9950 | 0.9950 | 0.9950 | 0.002 |
| 82 | 941-69-5 | 0.9955 | 0.9955 | 0.9955 | 0.9955 | 0.9955 | 0.9955 | 0.9955 | 0.9954 | 0.9950 | 0.9943 | 0.0019 |
| 83 | 94361-06-5 | 0.9921 | 0.9921 | 0.9921 | 0.9921 | 0.9920 | 0.9918 | 0.9901 | 0.9861 | 0.7296 | 0.4747 | 0.0019 |

| ID | CAS | F (0.001 mg) | F (0.01 mg) | F (0.1 mg) | F (1 mg) | F (5 mg) | F (10 mg) | F (50 mg) | F (100 mg) | F (500 mg) | F (1000 mg) | $K_e$ ($min^{-1}$) |
|---|---|---|---|---|---|---|---|---|---|---|---|---|
| 84 | 97-77-8 | 0.8355 | 0.8354 | 0.8347 | 0.8281 | 0.7985 | 0.7624 | 0.5412 | 0.3939 | 0.1343 | 0.0775 | 0.0024 |
| 85 | 98-51-1 | 0.9778 | 0.9778 | 0.9777 | 0.9768 | 0.9724 | 0.9661 | 0.8818 | 0.7463 | 0.3045 | 0.1811 | 0.0024 |
| 86 | 989-38-8 | 0.9518 | 0.9518 | 0.9515 | 0.9488 | 0.9359 | 0.9175 | 0.7391 | 0.5641 | 0.2002 | 0.1162 | 0.00041 |

**Figure S2:** Bioavailabilities as predicted by the ACD/Labs software for each of 86 EDC.

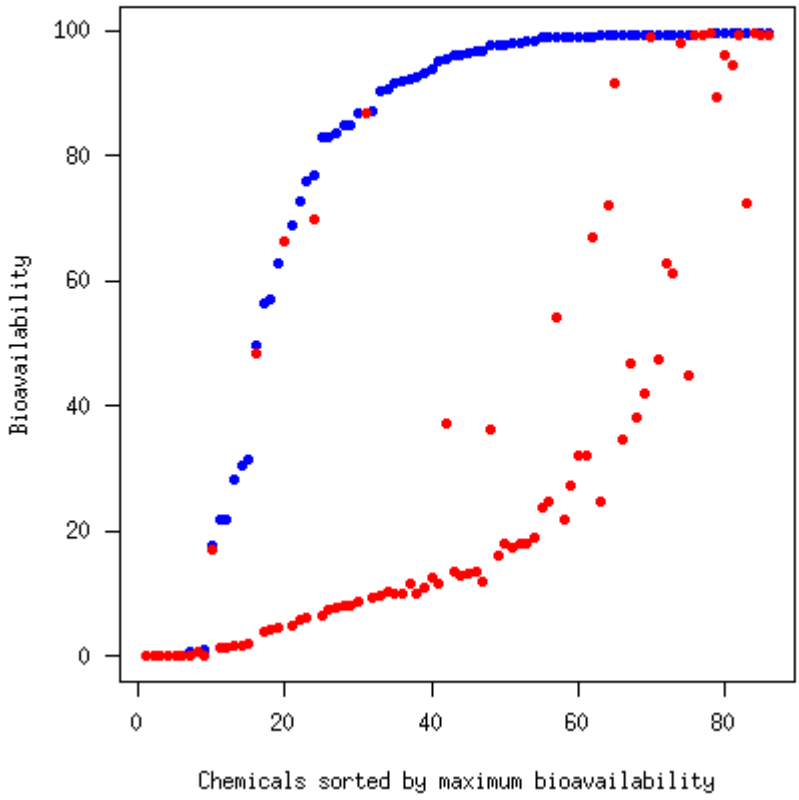


**Figure S2:** Bioavailability as predicted by ACD/Labs for each of 86 chemicals. The blue and red dots show respectively the bioavailability for oral administration of 0.001 mg and 1000 mg of each chemical.

**Figure S3:** Histogram of the half-life of each of the 86 EDC.

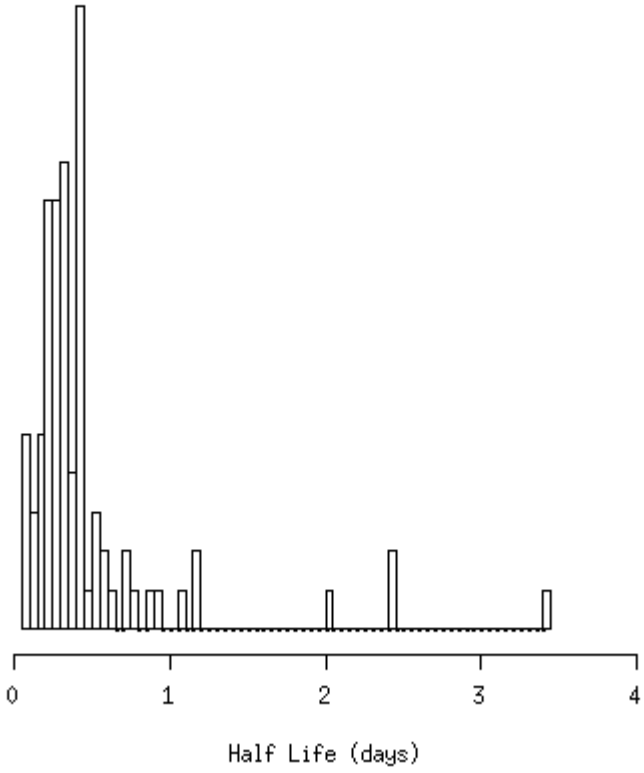


**Figure S3:** Histogram of the half life of each of the 86 chemicals, calculated from the total body clearance rate constant predicted by ACD/Labs.

**Figure S4:** Internal concentration *vs*. exposure rate for of each of the 86 EDC studied.

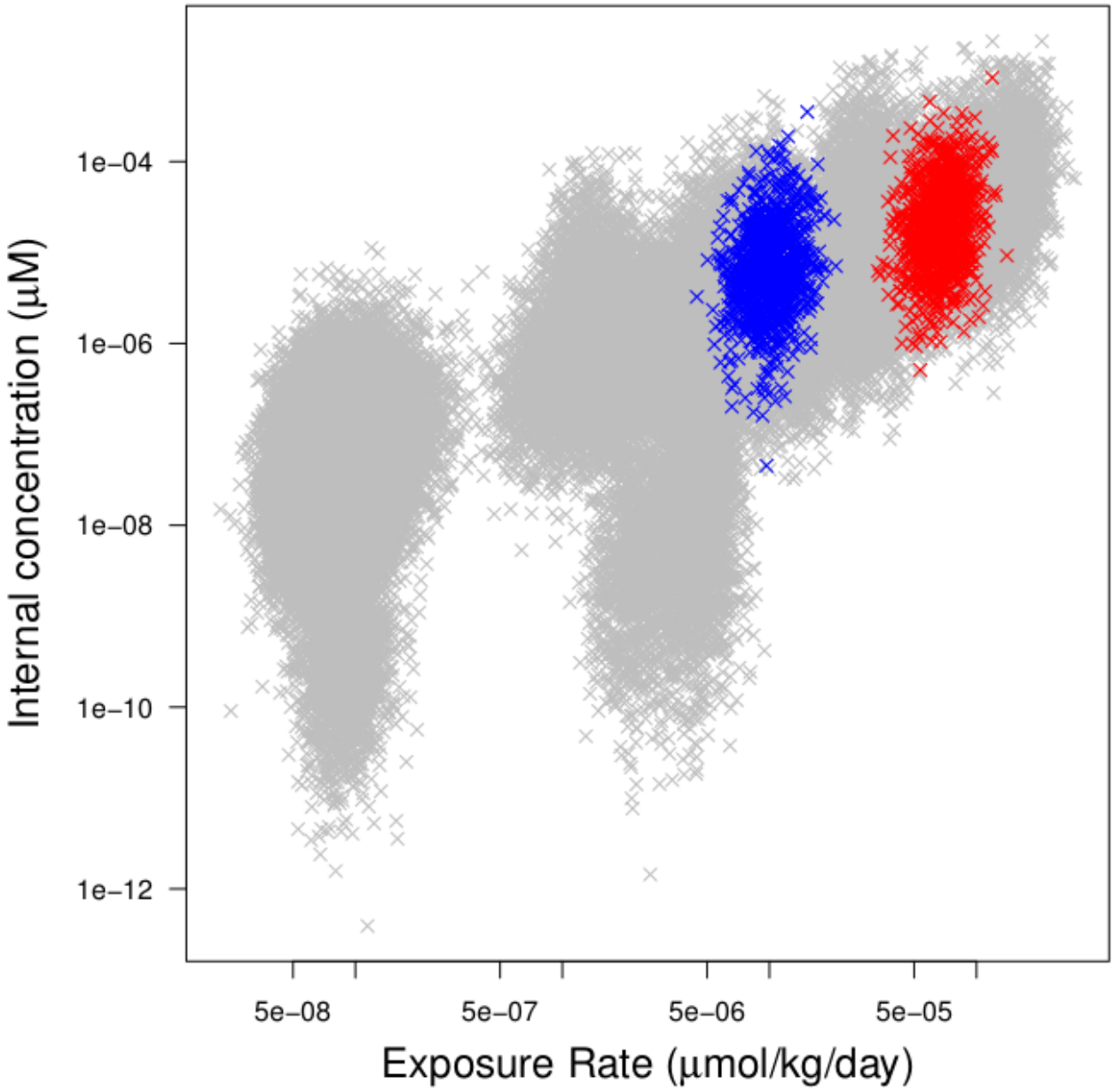


**Figure S4:** Steady-state internal concentrations of the 86 chemicals studied as a function of exposure levels. Exposures and pharmacokinetic parameters were randomly sampled 10000 times for each chemical (see text), resulting in visible spread. Results for two of the chemicals are highlighted (anastrozole in blue and 4,4'-oxydianiline in red).

**Figure S5:** Example of a random internal exposure profile.

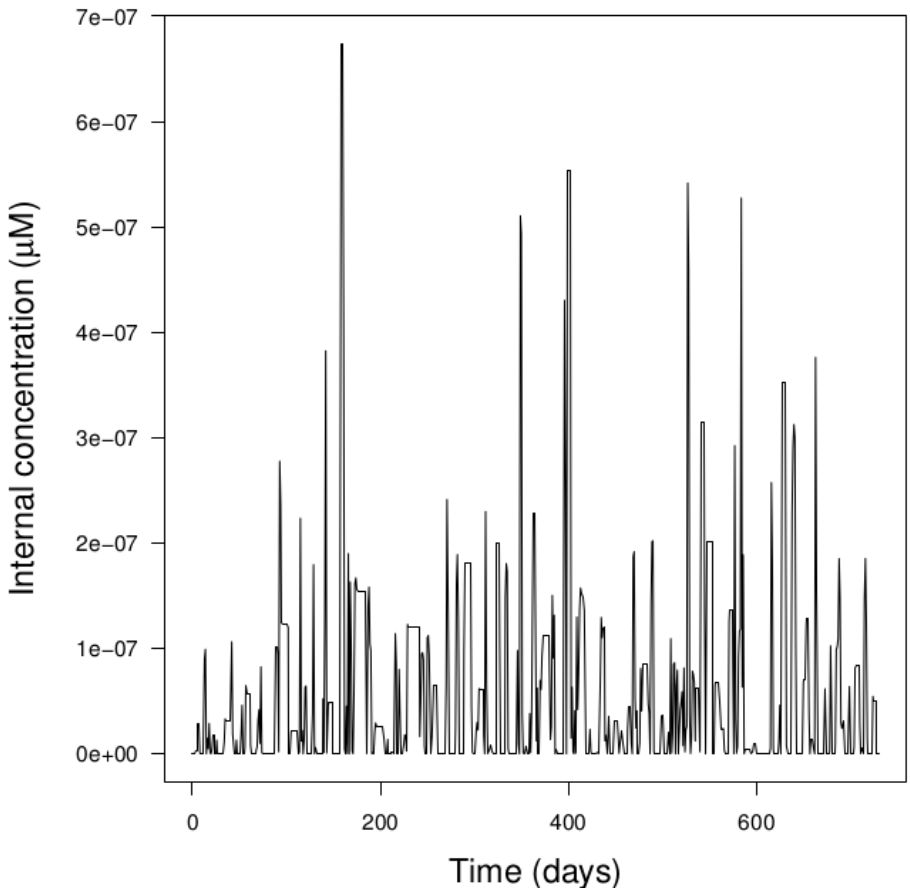


**Figure S5:** Example of a random internal exposure profile (for lindane). Exposure times and rates were Monte Carlo sampled. Internal exposure as a function of time was obtained by numerical integration of the one-compartment PK model.

**Figure S2:** Menstrual cycle model equations.

The equations of the menstrual cycle are adapted from Chen and Ward (2013), as indicated.

The differential equation for the dominant follicle mass (*F*) is a function of a background growth rate, a growth rate component stimulated by *FSH* according to Hill's model, and a degradation rate under *LH* control, also according to Hill's model:

$$\frac{\partial F}{\partial t} = \gamma_F + \frac{\beta_F \cdot F \cdot FSH^{m_6}}{EC_{FSH,F}^{m_6} + FSH^{m_6}} - \frac{\gamma_{\mathrm{F,R}} \cdot F^2 \cdot LH^{m_7}}{EC_{LH,F}^{m_7} + LH^{m_7}} \quad (1)$$

The ruptured follicle or scar mass (*R*) is formed from *F* degradation, with first and converted to *corpus luteum* (*C*):

$$\frac{\partial R}{\partial t} = \frac{\gamma_{\mathrm{F,R}} \cdot F^2 \cdot LH^{m_7}}{EC_{LH,F}^{m_7} + LH^{m_7}} - \gamma_{\mathrm{R,C}} \cdot R \quad (2)$$

The differential equation for *corpus luteum* mass is a function of its formation rate from *R*, and first order degradation:

$$\frac{\partial C}{\partial t} = \gamma_{\mathrm{R,C}} \cdot R - \delta_C \cdot C \quad (3)$$

The initial quantities of estradiol (*E2*, in nanograms) and progesterone (*P4*, in nanomoles) in blood and ovaries are given by:

$$Q_{\mathrm{E2},b}(t=0) = 60 \cdot V_{blood} \quad (4)$$

$$Q_{\mathrm{P4},b}(t=0) = 10 \cdot V_{blood} \quad (5)$$

$$Q_{\mathrm{E2},o}(t=0) = 4000 \cdot V_{ovary} \quad (6)$$

$$Q_{\mathrm{P4},o}(t=0) = 1200 \cdot V_{ovary} \quad (7)$$

The concentration of *E2* (nanograms/L) and *P4* (nanomoles/L) in blood and ovaries are:

$$C_{\mathrm{E2},b} = Q_{\mathrm{E2},b} \,/\, V_{blood} \quad (8)$$

$$C_{\mathrm{E2},o} = Q_{\mathrm{E2},o} \,/\, V_{ovary} \quad (9)$$

$$C_{\mathrm{P4},b} = Q_{\mathrm{P4},b} \,/\, V_{blood} \quad (10)$$

$$C_{\mathrm{P4},o} = Q_{\mathrm{P4},o} \,/\, V_{ovary} \quad (11)$$

*GnRH* (arbitrary units) is promoted by blood *E2*, and inhibited by blood *P4*, according to Hill's models:

$$Gn = \frac{\mathrm{E2}_b^{m_1}}{EC_{\mathrm{E2},Gn}^{m_1}+\mathrm{E2}_b^{m_1}} \cdot \frac{EC_{\mathrm{P4},Gn}^{m_2}}{EC_{\mathrm{P4},Gn}^{m_2}+\mathrm{P4}_b^{m_2}} \quad (12)$$

The blood *FSH* concentration (in µg/L) in under positive control by past values of *GnRH* ($\tau_{FSH}$ days before) and negative control by current *E2*, according to Hill's models:

$$FSH = \left(FSH_{min} + \frac{(FSH_{max}-FSH_{min})\cdot Gn_{(t-\tau_{FSH})}^{m_3}}{EC_{Gn_{FSH}}^{m_3} + Gn_{(t-\tau_{FSH})}^{m_3}}\right) \cdot \frac{EC_{\mathrm{E2}_{FSH}}^{m_4}}{EC_{\mathrm{E2}_{FSH}}^{m_4}+\mathrm{E2}_b^{m_4}} \quad (13)$$

The blood *LH* concentration (in µg/L) in under positive control by past values of *GnRH* ($\tau_{LH}$ days before), according to Hill's model:

$$LH = LH_{min} + \frac{(LH_{max}-LH_{min})\cdot Gn_{(t-\tau_{LH})}^{m_5}}{EC_{Gn_{LH}}^{m_5} + Gn_{(t-\tau_{LH})}^{m_5}} \quad (14)$$

The differential equation for *E2* quantity in blood is a function of transport to and from the ovaries, extra-ovarian production, and elimination rates:

$$\frac{\partial Q_{E2,b}}{\partial t} = F_{ovary}\left(C_{\mathrm{E2},o} - C_{\mathrm{E2},b}\right) + Kp_{\mathrm{E2}} \cdot \beta_{\mathrm{E2}} - Ke_{\mathrm{E2}} \cdot C_{\mathrm{E2},b} \quad (15)$$

The differential equation for *E2* quantity in the ovaries is as a function of its transport to and from blood, and its follicular and luteal production, which can be both affected by endocrine disruption (*ED*):

$$\frac{\partial Q_{\mathrm{E2},o}}{\partial t} = ED_{\mathrm{cyp19}} \cdot Kp_{\mathrm{E2}} \cdot \left(\beta_{\mathrm{E2}F} \cdot F + \beta_{\mathrm{E2}C} \cdot C\right) - F_{ovary}\left(C_{\mathrm{E2},o} - C_{\mathrm{E2},b}\right) \quad (16)$$

The differential equation for the quantity of *P4* in blood is a function of its transport to and from the ovaries, extra-ovarian production, and elimination rates:

$$\frac{\partial Q_{\mathrm{P4},b}}{\partial t} = F_{ovary}\left(C_{\mathrm{P4},o} - C_{\mathrm{P4},b}\right) + Kp_{\mathrm{P4}} \cdot \beta_{\mathrm{P4}} - Ke_{\mathrm{P4}} \cdot C_{\mathrm{P4},b} \quad (17)$$

The differential equation for the quantity of *P4* in the ovaries is a function of transport to and from blood, and luteal production:

$$\frac{\partial Q_{\mathrm{P4},o}}{\partial t} = Kp_{\mathrm{P4}} \cdot \beta_{\mathrm{P4C}} \cdot C - F_{ovary}\left(C_{\mathrm{P4},o} - C_{\mathrm{P4},b}\right) \quad (19)$$

**Table S3.** Menstrual cycle parameter values. Value are from Chen and Ward (2013), except were indicated.

| Parameter | Symbol | Value (units) |
|---|---|---|
| Ratio of disrupted over control *E2* synthesis | $ED_{CYP19}$ | - [a] |
| Time delay for *GnRH* control of *FSH* | $\tau_{FSH}$ | 1 (day) |
| Time delay for *GnRH* control of L*H* | $\tau_{LH}$ | 1.4 (day) |
| Baseline *E2* concentration | $\beta_{E2}$ | 0.1 (ng/L) |
| Follicular contribution to *E2* synthesis | $\beta_{E2,F}$ | 0.48 (ng/L/mass of *F*) |
| Luteal contribution to *E2* synthesis | $\beta_{E2,C}$ | 0.36 (ng/L/mass of *F*) |
| *E2* clearance from blood | $K_{e,E2}$ | 1600 (L/day) |
| *E2* synthesis scale factor | $K_{p,E2}$ | 1600 (L/day) |
| Baseline *P4* concentration | $\beta_{P4}$ | 0 (nmol/L) |
| Luteal contribution to *P4* synthesis | $B_{P4,C}$ | 0.12 (nmol/L/mass of *C*) |
| *P4* clearance from blood | $K_{e,P4}$ | 3621 (L/day) [b] |
| *P4* synthesis scale factor | $K_{p,P4}$ | 3621 (L/day) |
| *E2* $EC_{50}$ for *GnRH* secretion promotion | $EC_{E2,Gn}$ | 185 (ng/L) |
| *E2* Hill exponent for *GnRH* secretion | $m_1$ | 2 (unitless) |
| *P4* $EC_{50}$ for *GnRH* secretion inhibition | $EC_{P4,Gn}$ | 10 (nmol/L) |
| *P4* Hill exponent for *GnRH* secretion inhibition | $m_2$ | 2 (unitless) |
| *GnRH* $EC_{50}$ for *FSH* secretion promotion | $EC_{Gn,FSH}$ | 0.453 (arbitrary units) |
| *GnRH* Hill exponent for *FSH* secretion promotion | $m_3$ | 2 (unitless) |
| *E2* $EC_{50}$ for *FSH* secretion inhibition | $EC_{E2,FSH}$ | 432 (ng/L) |
| *E2* Hill exponent for *FSH* secretion inhibition | $m_4$ | 4 (unitless) |
| Minimum *FSH* concentration | $FSH_{min}$ | 28.5 (μg/L) |
| Maximum *FSH* concentration | $FSH_{max}$ | 500 (μg/L) |
| *GnRH* $EC_{50}$ for *LH* release | $EC_{Gn,LH}$ | 0.447 (arbitrary units) |
| *GnRH* Hill exponent for *LH* release | $m_5$ | 10 (unitless) |
| Minimum *LH* concentration | $LH_{min}$ | 36.4 (μg/L) |

| | | |
|---|---|---|
| Maximum *LH* concentration | $LH_{max}$ | 676 (µg/L) |
| Baseline follicle growth rate | $\gamma_F$ | 0 (arbitrary units/day) |
| *FSH* $EC_{50}$ for follicle growth stimulation | $EC_{FSH,F}$ | 150 (µg/L) |
| *FSH* Hill exponent for follicle growth stimulation | $m_6$ | 2 (unitless) |
| *FSH* enhanced follicle growth stimulation rate constant | $\beta_F$ | 2.1 (1/day) |
| *LH* $EC_{50}$ for follicle rupture | $EC_{LH,F}$ | 325 (µg/L) |
| *LH* Hill exponent for follicle rupture | $m_7$ | 2 (unitless) |
| Follicle rupture rate constant per unit follicle mass | $\gamma_{F,R}$ | 0.06 (1/day/arbitrary units) |
| *R* to *C* conversion rate constant | $\gamma_{R,C}$ | 0.285 (1/day) |
| *Corpus luteum* decay rate constant | $\delta_C$ | 0.345 (1/day) |
| Blood volume | $V_{blood}$ | 4.1 (L) [c] |
| Ovaries volume | $V_{ovary}$ | 0.2 (L) [c] |
| Ovaries blood flow | $F_{ovary}$ | 30 (L/day) [c] |

[a] The value of this parameter depends on exposure to endocrine disrupting chemicals.

[b] Little et al. (1966).

[c] International Commission on Radiological Protection (ICRP) (2002).

**Table 4:** Menstrual cycle initial state variables' values.

| State variable | Symbol | Value (units) |
|---|---|---|
| Dominant follicle mass | $F$ | 79.48 (arbitrary units) |
| Ruptured follicle (scar) mass | $R$ | 20.23 (arbitrary units) |
| *Corpus luteum* mass | $C$ | 33.35 (arbitrary units) |
| Quantity of estradiol in blood | $Q_{E2,b}$ | 206.1 (ng) |
| Quantity of estradiol in ovaries | $Q_{E2,o}$ | 545.1 (ng) |
| Quantity of progesterone in blood | $Q_{P4,b}$ | 16.43 (nmol) |
| Quantity of progesterone in ovaries | $Q_{P4,o}$ | 97.53 (nmol) |

**Figure S6:** Simulation of normal ovarian cycling and comparison to data.

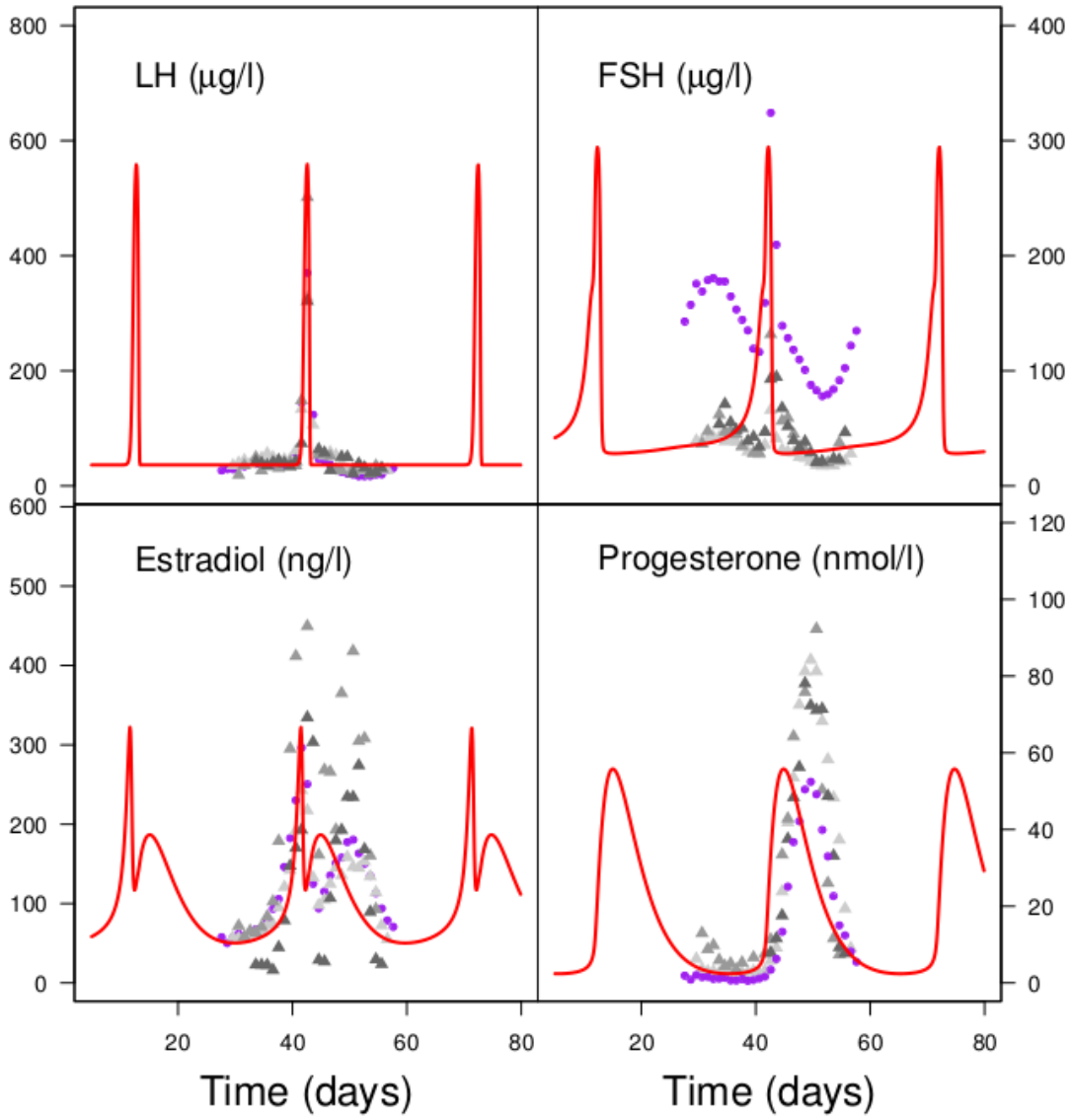


**Figure S6:** Model simulated time course of *LH*, *FSH*, *E2* and *P4* during normal human ovarian cycles (red lines). The model equations and parameter values used are given in Methods S2 and Tables S3 and S4 above. Data are overlaid as points: purple circles from McLachlan et al. (1990, Fig. 1); gray triangles from Welt et al. (1999). The LH data points from Welt *et al*. were rescaled so that their baseline values match with those of McLachlan et al. The same rescaling factor was applied to Welt et al. FSH data.

**Figures S7-S10:** Simulation of normal and perturbed ovarian cycling.

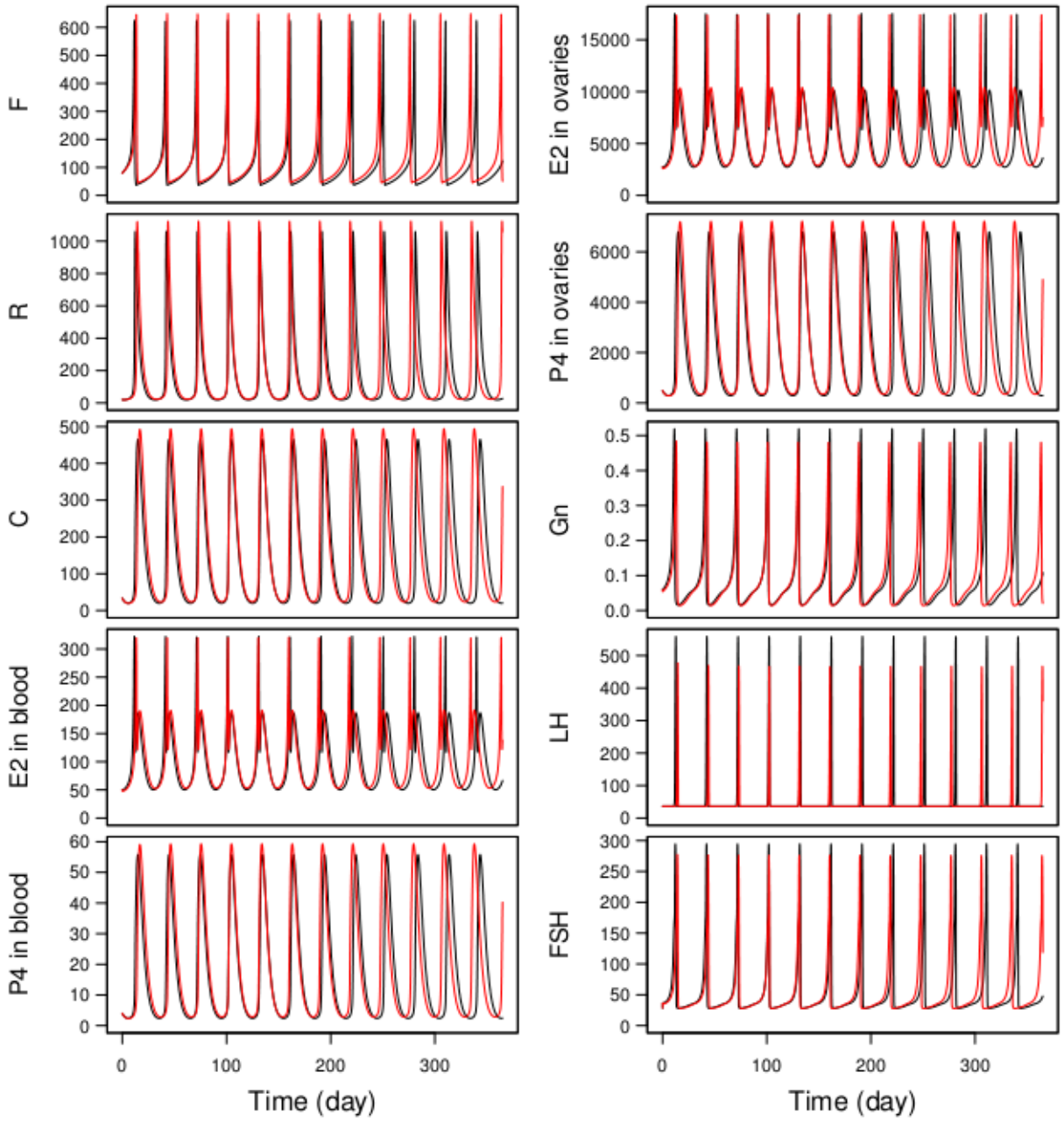


**Figure S7:** Simulated time course of all model variables during normal ovarian cycles (parameter $ED_{CYP19}$ set to 1, black lines) and with a 5% constant inhibition of aromatase (parameter $ED_{CYP19}$ set to 0.95). The model equations and parameter values used are given in Methods S2 and Tables S3 and S4 above. *LH* and *FSH* units are in µg/L. *GnRH* units are arbitrary, the units of the other variables are given in Table S4 above. The perturbed cycle differs only slightly from normal.

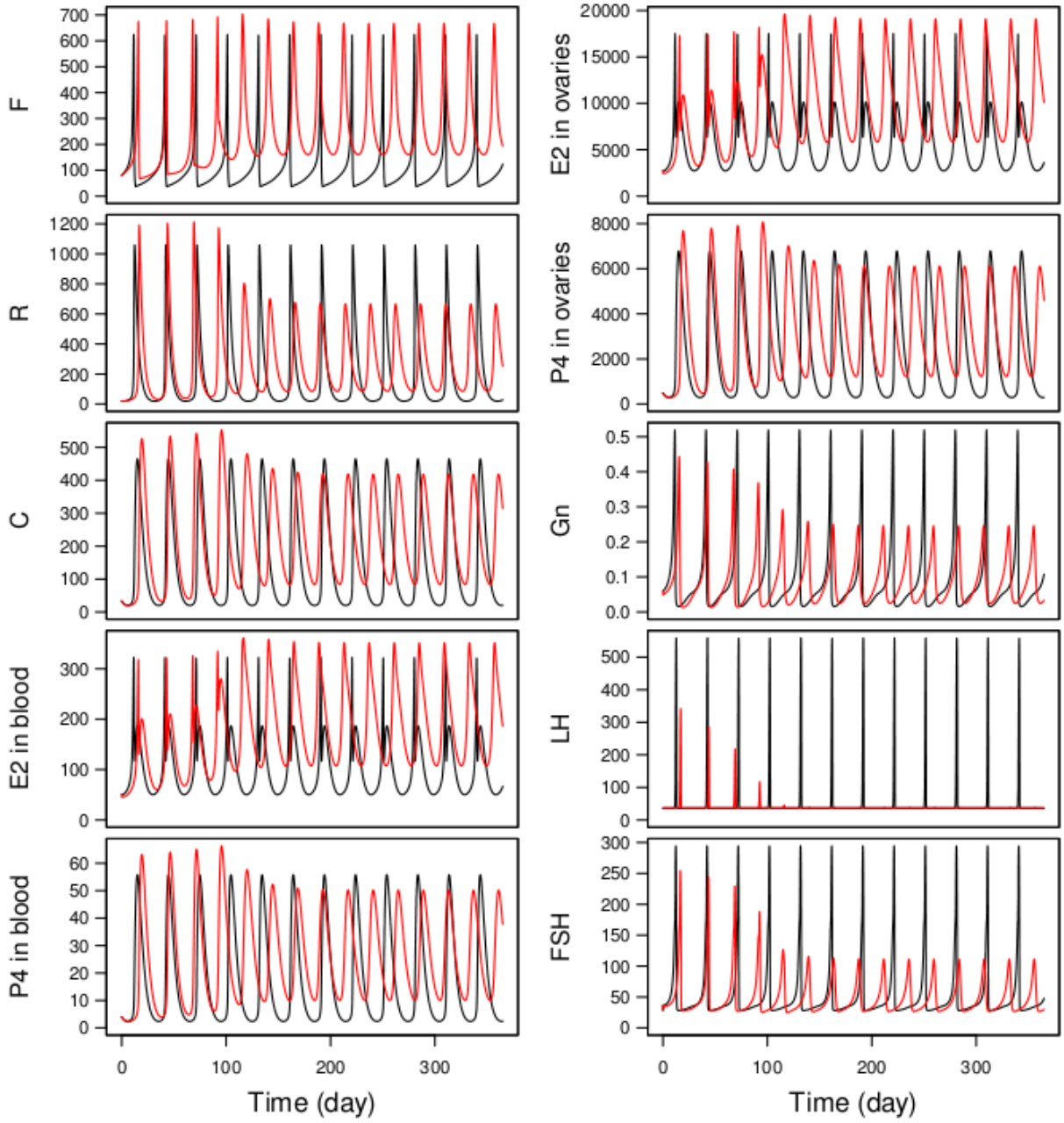


**Figure S8:** Simulated time course of all model variables during normal ovarian cycles (parameter $ED_{CYP19}$ set to 1, black lines) and with A 10% constant inhibition of aromatase (parameter $ED_{CYP19}$ set to 0.9). The model equations and parameter values used are given in Methods S2 and Tables S3 and S4 above. *LH* and *FSH* units are in µg/L. *GnRH* units are arbitrary, the units of the other variables are given in Table S4 above. LH peaks disappear rapidly and the systems bifurcates to a new solution.

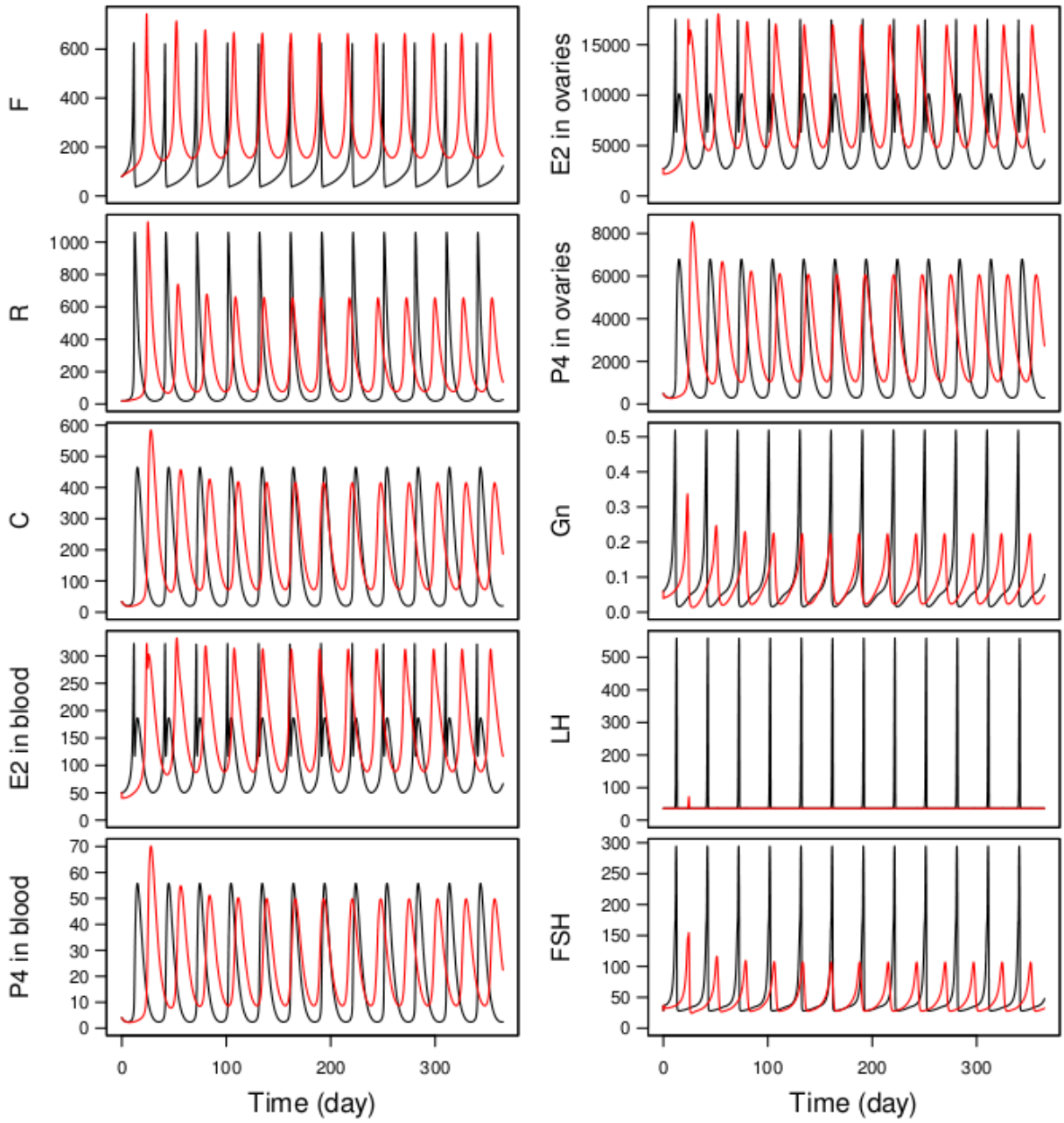


**Figure S9:** Simulated time course of all model variables during normal ovarian cycles (parameter $ED_{CYP19}$ set to 1, black lines) and with A 20% constant inhibition of aromatase (parameter $ED_{CYP19}$ set to 0.8). The model equations and parameter values used are given in Methods S2 and Tables S3 and S4 above. *LH* and *FSH* units are in µg/L. *GnRH* units are arbitrary, the units of the other variables are given in Table S4 above. The cycle is profoundly disrupted.

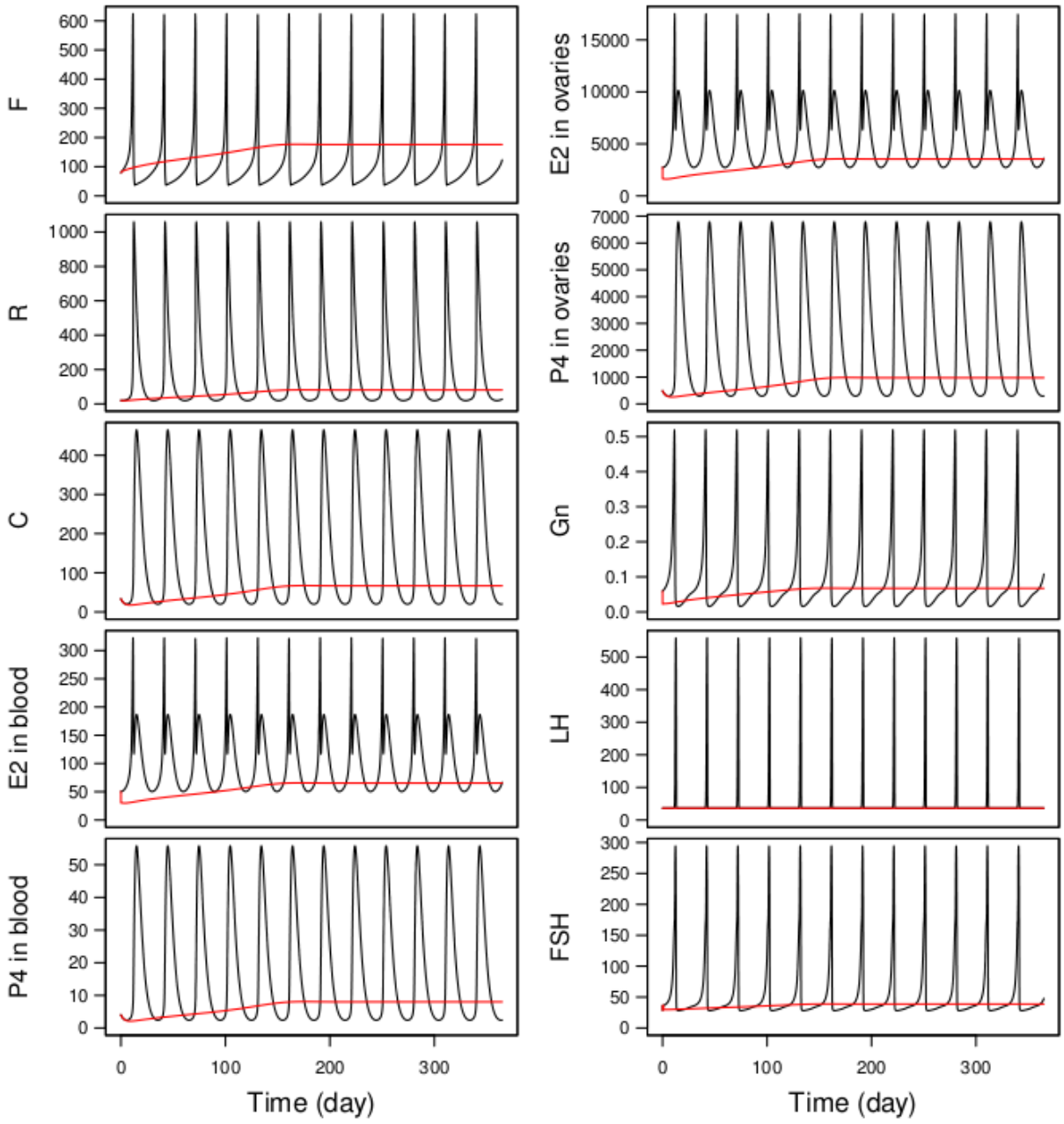


**Figure S10:** Simulated time course of all model variables during normal ovarian cycles (parameter $ED_{CYP19}$ set to 1, black lines) and with A 40% constant inhibition of aromatase (parameter $ED_{CYP19}$ set to 0.6). The model equations and parameter values used are given in Methods S2 and Tables S3 and S4 above. *LH* and *FSH* units are in µg/L. *GnRH* units are arbitrary, the units of the other variables are given in Table S4 above. The cycle is totally disrupted.

Figure S**11**: Simulation of estradiol time profiles during time-varying exposures to 86 EDCs.

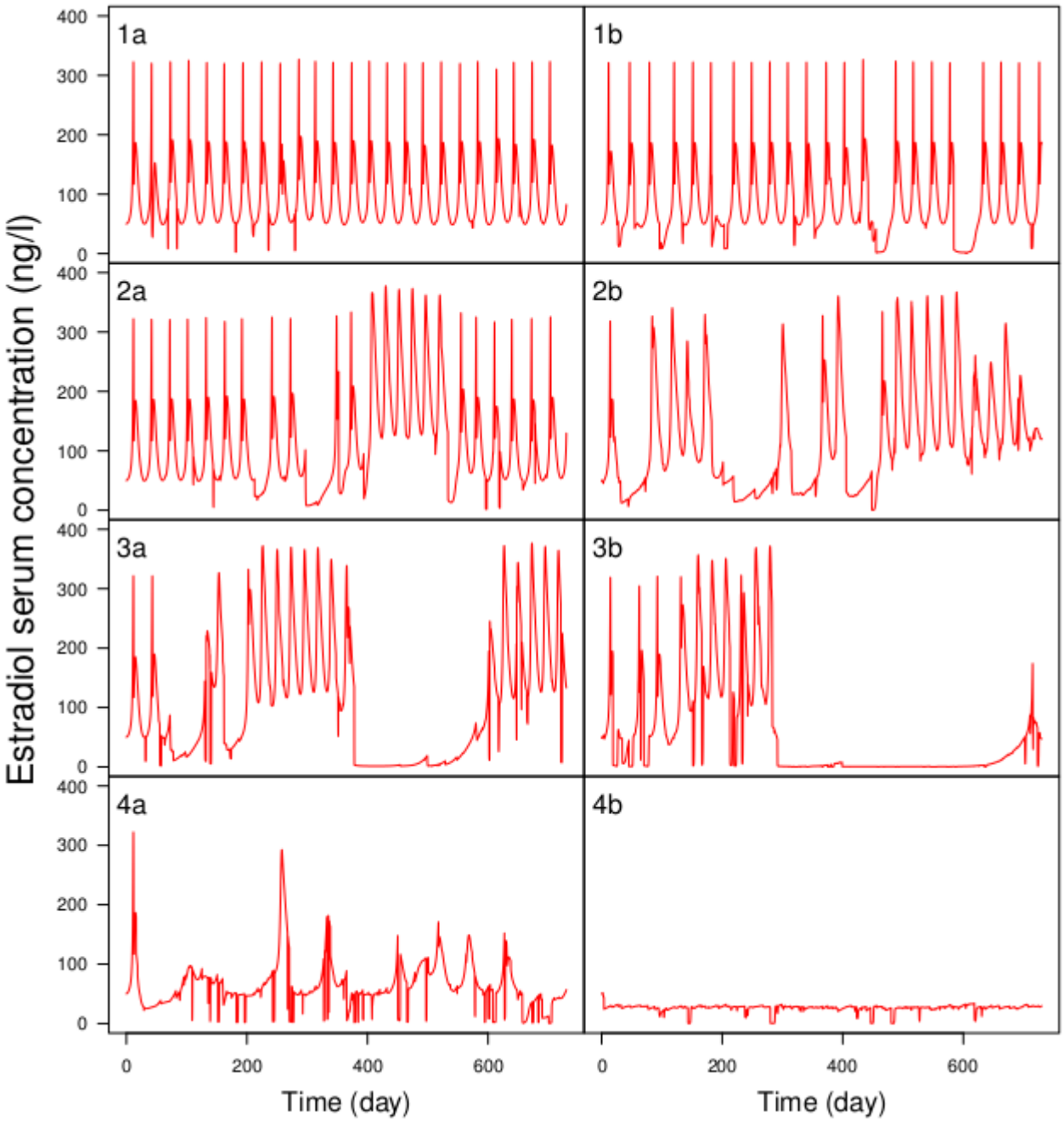


**Figure S11:** Typical simulated time profiles of estradiol concentration during time-varying exposures to random mixtures of 86 aromatase inhibitors. Four classes (rows) of increasing disruption are illustrated (see main text). Left column: least disrupted profile in its class; Right column: most disrupted. Panel 1a shows a practically normal profile with regular ovulation peaks. Panel 4b shows complete disruption.

**References**

Chen CY, Ward JP. 2013. A mathematical model for the human menstrual cycle. Math. Med. Biol. 31:65–86; doi:10.1093/imammb/dqs048.

International Commission on Radiological Protection (ICRP). 2002. Basic anatomical and physiological data for use in radiological protection: reference values. ICRP Publication 89. Ann. ICRP 32(3/4).

Little B, Tait JF, Tait SA, Erlenmeyer F. 1966. The metabolic clearance rate of progesterone in males and ovariectomized females. J. Clin. Invest. 45:901–912; doi:10.1172/JCI105405.

McLachlan RI, Cohen NL, Dahl KD, Bremner WJ, Soules MR. 1990. Serum inhibin levels during the periovulatory interval in normal women: relationships with sex steroid and gonadotrophin levels. Clin. Endocrinol. (Oxf.) 32: 39–48.

Parrot N, Lavé T. 2002. Prediction of intestinal absorption: comparative assessment of GASTROPLUS and IDEA. Eur. J. Pharm. Sci. 17: 51–61.

Welt CK, McNicholl DJ, Taylor AE, Hall JE. 1999. Female reproductive aging is marked by decreased secretion of dimeric inhibin. J. Clin. Endocrinol. Metab. 84:105–111; doi:10.1210/jcem.84.1.5381.